LA-UR- 97-3627

*Approved for public release; distribution is unlimited.*

Title: Neutronic Design of the APT Target/Blanket

CONF-971125--

Author(s): E.J. Pitcher
G.J. Russell
R.B. Kidman
P.D. Ferguson
M. Todosow, BNL

Submitted to: November 16-20, 1997
Embedded Topical on Nuclear Applications of Accelerator Technology
Albuquerque, NM



**Los Alamos**
NATIONAL LABORATORY

## DISCLAIMER

# NEUTRONIC DESIGN OF THE APT TARGET/BLANKET

E.J. Pitcher, G.J. Russell, R.B. Kidman, and P.D. Ferguson
Los Alamos National Laboratory
P.O. Box 1663, MS H813
Los Alamos, New Mexico 87545
(505)665-0651

M. Todosow
Brookhaven National Laboratory
Building 179d
Upton, New York 11973
(516)344-2445

## ABSTRACT

The primary function of the Accelerator Production of Tritium Target/Blanket assembly is the safe and efficient production of tritium. The T/B accepts a 1.7-GeV, 100-mA proton beam and produces neutrons via the spallation process. These neutrons then react with $^3$He to produce tritium. Neutronic optimization of the T/B is achieved by efficiently using the proton beam to produce neutrons and then, once produced, assuring that they are captured mostly by $^3$He. This optimization must occur within the constraints imposed by engineering considerations such as heat flux limits, structural integrity, fabricability, and safe and reliable operation. The target/blanket achieves these goals with a neutron production rate that is 75% of that achievable with an ideal target, and a neutronic efficiency of 84%, leading to an overall tritium production rate that is 63% of the theoretical maximum.

## I. INTRODUCTION

The primary function of the Accelerator Production of Tritium (APT) Target/Blanket (T/B) assembly is the safe and efficient production of tritium. Neutronic performance is a primary factor driving the design of the T/B. The principal figure of merit with respect to neutronic performance is the tritium production rate, or the number of tritium atoms produced per proton incident on target (T/p). This is, in turn, a product of two quantities: the neutrons produced per proton incident on target (n/p), and the efficiency with which these neutrons are captured by $^3$He to produce tritium (T/n). Neutronic optimization seeks to maximize both n/p and T/n.

The neutron production rate, n/p, is a function of the proton energy $E_p$ and the target material and geometry. For proton energies greater than a few hundred MeV and an infinite tungsten target in which the beam is launched 0.5 m downstream of the front face (nearly eliminating front-surface leakage), the relation

$$\frac{n}{p}\left(E_p\right) = 42.3\left(E_p - 0.21\right), \qquad (1)$$

can be used to predict neutron yield, where $E_p$ has units of GeV. Note that the yield is nearly linear with proton energy with a 210-MeV offset. For a highly-reentrant, pure tungsten target, one can expect about 63 neutrons produced per 1.7-GeV proton incident on target. The energy spectrum of these neutrons, shown in Figure 1, has two components, which is a result of the spallation process by which they are produced. In the first stage of spallation, called the intranuclear cascade phase, a high-

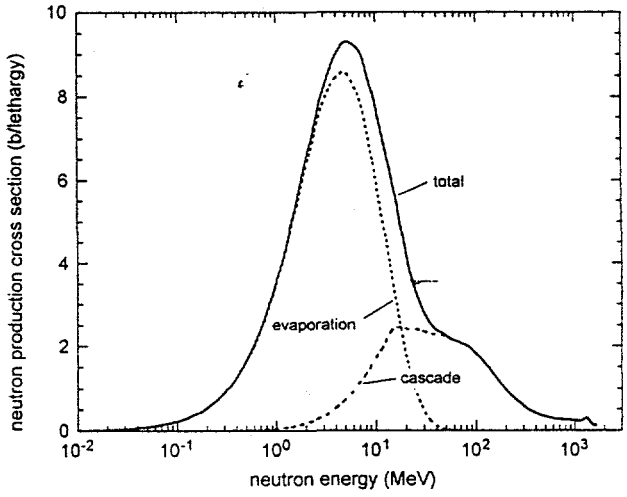


Figure 1. Energy spectrum of neutrons produced by 1.7-GeV protons incident on a thin tungsten target.

energy proton interacts with an individual nucleon within the nucleus and may eject neutrons with energies up to the incident proton energy. This produces the high-energy tail on the spectrum, evident in Figure 1. In the second stage of spallation, the highly-excited nucleus relaxes through a process termed "evaporation," in which neutrons are emitted (nearly) isotropically with a broad range of energies up to several tens of MeV. It is primarily these evaporation neutrons that are moderated and then captured in $^3$He to produce tritium. In a thin target where only the incident protons interact, about a fourth of the neutrons are produced in the cascade phase while three-fourths are generated in the evaporation phase. For a sufficiently thick target, however, nearly all (some fraction inevitably escapes) cascade neutrons interact with the target, generating additional evaporation neutrons.

Optimization of the neutronic efficiency, or T/n, is achieved by minimizing the use of strong and moderate neutron absorbers (other than $^3$He) within the T/B, and by neutronically decoupling the tungsten target, a moderate neutron absorber, from the blanket. This feature will be described in more detail later.

## II. THE LAHET CODE SYSTEM AND CINDER'90

The nuclear processes that take place in the T/B are simulated using the LAHET Code System[1] (LCS). This powerful suite of codes models the spallation process and particle transport via the Monte Carlo technique. It is composed primarily of two codes, LAHET and MCNP.[2] LAHET is a model-based Monte Carlo transport code that simulates the spallation process and transport of all charged particles and neutrons with energies greater than 20 MeV. Neutrons with energies less than 20 MeV and photons of all energies are handled by the data-based Monte Carlo transport code MCNP. These codes are used to predict T/p, particle fluxes, energy deposition, spallation product generation rates, and damage parameters (e.g., dpa's, gas production). Another code, CINDER'90,[3] is used to predict radionuclide inventories in the T/B as a function of time during operation of the APT facility.

## III. THE TARGET/BLANKET MODEL

The accuracy with which the LCS predicts neutronic performance of the T/B depends on the fidelity of the model provided by the user. Not only must the model be a faithful reproduction of the geometry, but the materials specifications must accurately represent reality in terms of quantity of structure and coolant, trace elements in alloys, etc. The geometry of the current model is depicted in Figures 2 through 4. The model includes all components of the T/B relevant to tritium production. Each of the

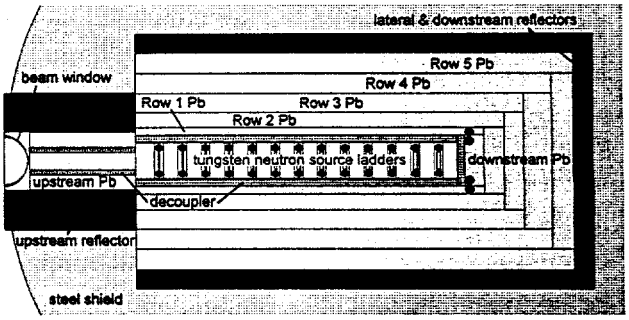


Figure 2. Top view of the T/B geometry.

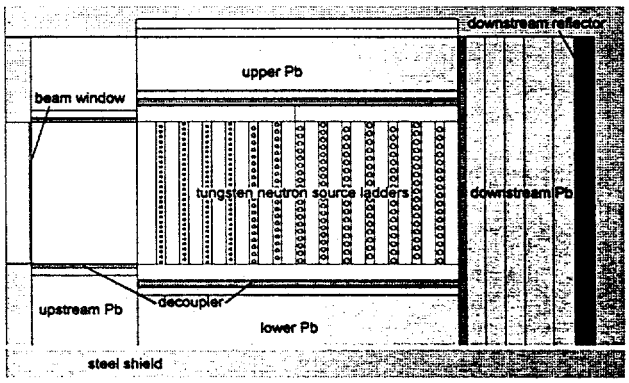


Figure 3. Side view of the T/B geometry.

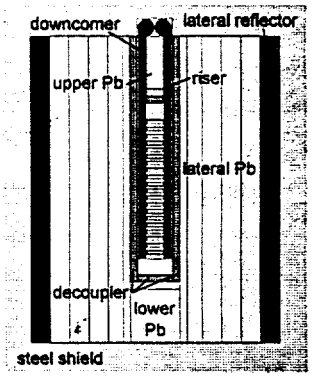


Figure 4. Front view of the T/B geometry.

thirteen ladders comprising the tungsten neutron source is modeled in great detail. The tungsten rods, Inconel-718 clad, and surrounding heavy-water coolant within each rung are homogenized in proportion to their specified volume fractions, while the stainless steel walls of the ladder housing are modeled explicitly. For ease of modeling and calculational expediency, the decoupler and lead blanket regions are modeled as homogeneous mixtures of their respective material constituents. Homogenization produces accurate results provided the particle mean free paths are greater than the characteristic dimensions of a "unit cell" comprising the region. This

approximation is valid for high-energy particles, but is less accurate for low-energy neutrons. Models of the blanket region in which the individual $^3$He-filled aluminum tubes surrounded by water have been modeled explicitly predict a T/p ratio that is about 3% below that predicted by equivalent homogeneous models.

Many trade studies have been performed to optimize the neutronic performance of the T/B. The results of some of these are presented below. It is worth noting that a 1% increase in T/p translates into annual savings in operating expense of approximately $600K and capital cost savings of approximately $20M.

## IV. TUNGSTEN NEUTRON SOURCE OPTIMIZATION

Due to its high-temperature characteristics and high thermal conductivity, tungsten is the material of choice for the primary target. Tungsten has a moderate thermal neutron absorption cross section (around 20 barns) and so the design of the primary target must minimize the interaction of thermal neutrons with tungsten.

### A. Target Geometry

For illustration purposes, let us consider neutron production and leakage from a stopping-length (30 cm) solid cylinder of tungsten with a 1-GeV proton beam traveling on the cylinder axis and incident on one of the flat faces. Figure 5 shows neutron production, leakage and absorption for a cylindrical tungsten target as a function of target diameter. At small diameters, production and leakage closely track one another as the mean free paths of the neutrons are longer than the characteristic dimensions of the target. As the target diameter approaches several mean free paths, absorption increases and, by a diameter of 20 cm, total neutron leakage peaks. Beyond this diameter fewer neutrons leak from the target even though total neutron production is still increasing. For target diameters larger than 1 m essentially all of the neutron leakage is from the front and back faces.

This study demonstrates that neutron leakage from a solid tungsten target is maximum when the characteristic transverse dimensions of the tungsten target do not exceed about 20 cm. Unfortunately, a 20 cm by 20 cm tungsten target cannot practically withstand a proton beam with power in the 100-MW range, as needed by APT to meet production requirements. Instead, the 20-cm length is preserved in one dimension while the other dimension is allowed to grow to an extent that yields acceptable power densities in the tungsten. This philosophy has led to a tungsten neutron source that is 22 cm wide by 180 cm high.

Neutron leakage from the tungsten is further enhanced by segmentation along the direction of proton beam propagation. Figure 6 shows the enhanced leakage gained by segmenting the target. It shows neutron leakage from a cylindrical tungsten target increases from about 58% of total neutron production for a solid target to better than

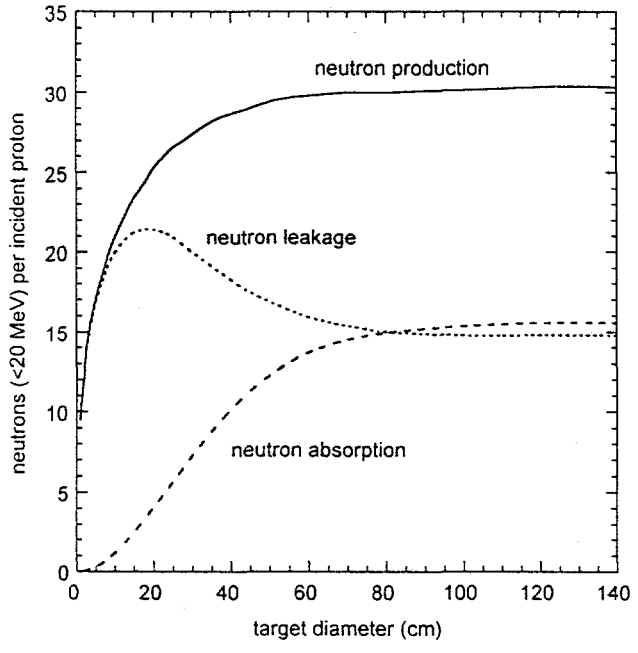


Figure 5. Neutron production, leakage, and absorption for a 30-cm-long cylindrical tungsten target.

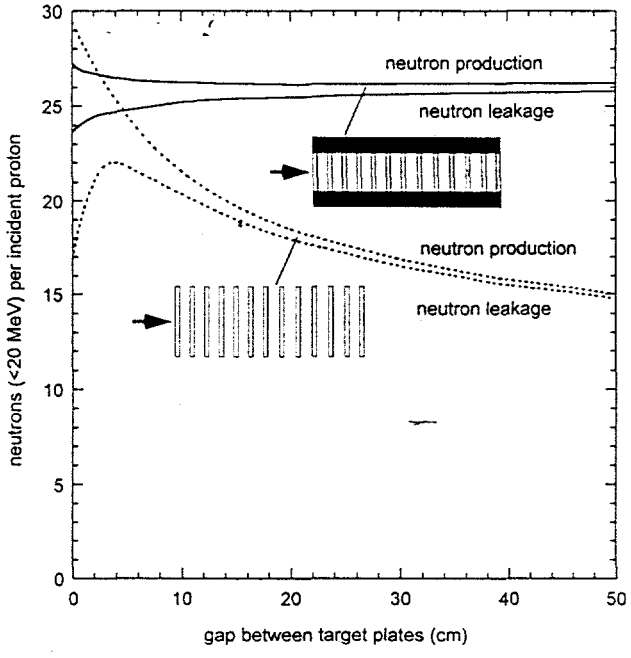


Figure 6. Neutron leakage gained by segmenting the target, and neutron production gained by adding a lateral blanket.

98% for the same target split into 13 disks with a 20-cm gap between each disk. Unfortunately, radial leakage of high-energy particles is also enhanced as the gap increases, and so total neutron production decreases. This is addressed by encasing the tungsten target by additional target material. Since this lateral target material is not subjected to the direct proton beam its power densities are much lower. Therefore, it makes sense to use lead here, since lead has a much lower neutron absorption cross section than tungsten. Figure 6 shows that when the split target with 20-cm gaps is encased by a 20-cm-thick annulus of lead, neutron leakage and neutron production both increase by almost 50%. These features of an axially-segmented tungsten target and encasement by a lateral lead blanket are incorporated in the T/B, where the tungsten is distributed in 13 ladders, and surrounded on all sides (except the front) by lead.

The thickness of the tungsten neutron source in the direction of proton beam propogation is sized to keep the peak power density in the downstream lead region below 100 W/cm$^3$. Figure 7 shows how the downstream lead peak power density varies with equivalent tungsten thickness in the neutron source region. This study indicates that a minimum thickness of 23 cm is required to meet the 100 W/cm$^3$ limit. It is this design criterion that sets the number of ladders at 13, which in the current design provides an equivalent tungsten thickness of 23.8 cm.

B. Tungsten Neutron Source Coolant

The mechanical design should seek to minimize the volume fraction of coolant in the tungsten neutron source because the coolant slows down the high-energy protons without producing many neutrons. Further, the coolant should not have strong neutron moderation properties as the design goal is to allow neutrons to leak from the tungsten neutron source with high energy and thereby minimize parasitic capture in the tungsten.

Two fluids were evaluated neutronically as coolant for the tungsten neutron souce: light water and heavy water. Light water is not expected to perform as well because neutrons will be strongly moderated and then absorbed in the tungsten. When the heavy water coolant in the tungsten neutron source is replaced by light water, calculations show the tritium production rate drops by approximately 9%. Thus heavy water is used to cool the tungsten neutron source.

C. Ladder Spacing

The spacing between ladders in the tungsten neutron source region influences the spatial distribution of neutron production. The greater the spacing, the greater the fraction of neutrons produced in the lead blanket and the lower the fraction produced in the tungsten neutron source. This is because a larger spacing allows more neutron-producing high-energy particles to escape laterally from the neutron source region and into the lead blanket region. Also, a larger spacing allows a higher fraction of neutrons produced in the tungsten to escape into the blanket region. Figure 8 shows how tritium production varies with ladder spacing. It shows tritium production peaking at a spacing of 25 cm. The present design has a spacing that is slightly larger, 30 cm, to allow space on the top of the tungsten neutron source modules for the layout of coolant pipes.

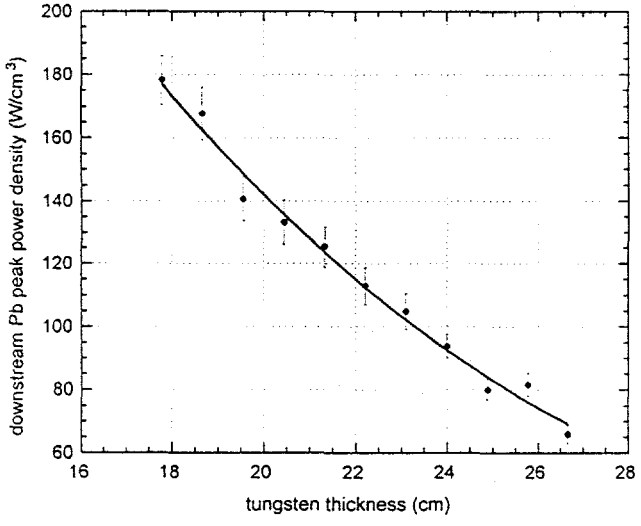


Figure 7. Peak power density in the downstream lead region as a function of tungsten thickness.

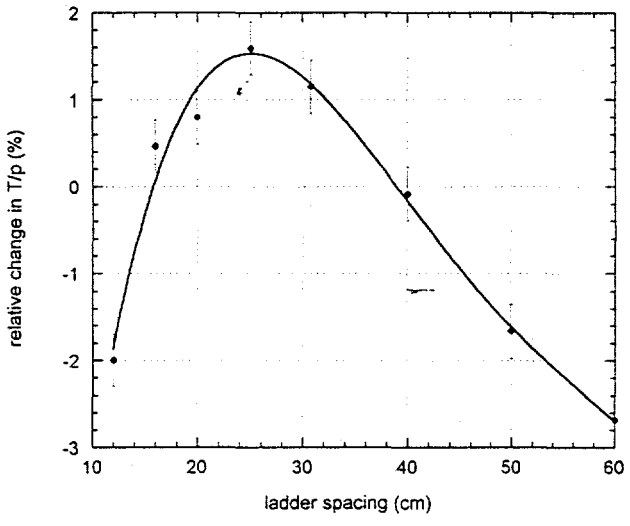


Figure 8. Sensitivity of tritium production on ladder spacing.

D. Ladder Downcomer Size

The diameter of the ladder downcomers and risers influences the distribution of flow among the ladder rungs. From a thermal-hydraulics viewpoint, larger downcomers are better as they reduce flow maldistribution. However, the presence of additional heavy water in the tungsten neutron source region that arises from increasing the downcomer diameter both reduces total neutron production and increases parasitic capture in the tungsten. Figure 9 shows how the tritium production rate varies with downcomer diameter. It shows that small increases in the downcomer diameter have a significant negative impact on the tritium production rate, and compels the thermal-hydraulic designers to seek alternative solutions to flow maldistribution, and not increase the downcomer diameter beyond its present design value of 8.89 cm.

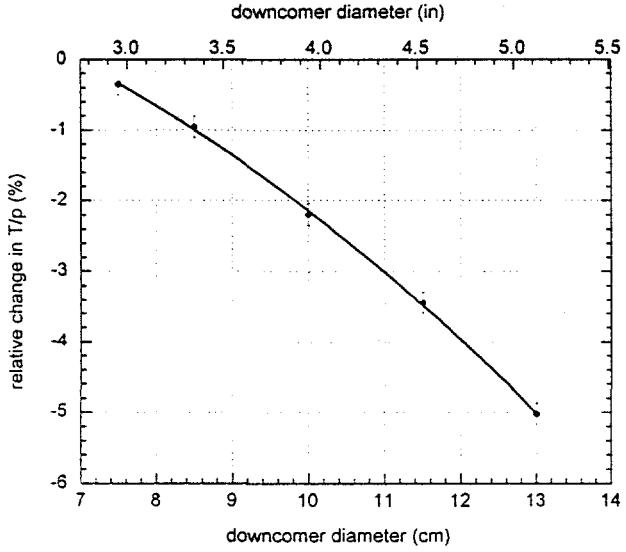


Figure 9. Sensitivity of T/p on the diameter of the ladder downcomers and risers.

## V. OPTIMIZATION OF THE DECOUPLER

A neutron decoupler region surrounds the tungsten neutron source, consisting of the lateral decoupler and the decoupler regions in the upstream and downstream blanket regions. In general, the decoupler's function is to be highly transparent for high-energy neutrons and other particles leaving the tungsten neutron source, but to preferentially absorb neutrons that scatter from the lead toward the tungsten neutron source.

A. Decoupler $^3$He Pressure

As the quantity of $^3$He through which a neutron must pass increases, so does its probability of capture. There are two ways in which $^3$He may be added to the decoupler. One is by making the decoupler region thicker (e.g., adding more tubes or increasing the tube diameter), and the other is by increasing the $^3$He pressure within the tubes. Increasing the decoupler thickness not only adds more $^3$He, but also more structure and coolant, which reduces neutron production in the blanket by slowing down high-energy particles passing through the decoupler. By increasing the pressure within the tubes, only $^3$He is added to the decoupler ($^3$He tube wall thickness is driven by external buckling pressure, not internal pressure) and consequently there is no loss in neutron production.

The dependence of the tritium production rate on the decoupler $^3$He pressure is shown in Figure 10. Compared to the present design pressure of 130 psia (assuming a $^3$He temperature of 400 K), an additional 0.5% gain in T/p may be realized by increasing the pressure to approximately 200 psia. An additional benefit derived from increased pressure is a drop in the fraction of tritium implanted in the tube walls.[4] This gain in T/p must be weighed against the attendant increase in $^3$He inventory in the T/B and the operational impacts of 200-psia operation.

B. Decoupler Thickness

The optimum decoupler thickness depends sensitively on its material composition. Aluminum structure should be kept to an absolute minimum, as its presence degrades the energy of particles scattered into the lead blanket and thereby reduces total neutron production. As it is desirable to strongly moderate any neutrons passing through the decoupler and capture them in the $^3$He prevalent in this region, light water is used to cool the aluminum structure. From a neutronic viewpoint, the quantity of light water

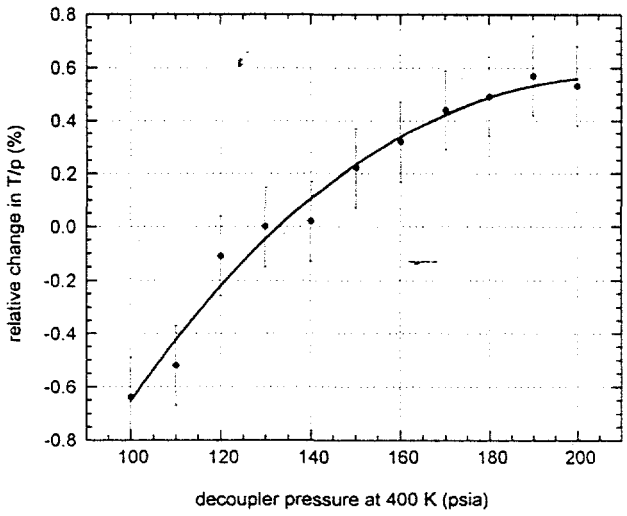


Figure 10. Sensitivity of T/p on $^3$He pressure in the decoupler.

should be optimizied for providing adequate neutron moderation; too much water will hurt total neutron production in the same way as aluminum. Figure 11 shows how T/p varies with decoupler thickness in the present design, which has 62% $^3$He, 27% light water, and 11% Al-6061 by volume. Tritium production peaks at a thickness of about 7 cm. Lower fractions of aluminum and water will push this optimum toward a thicker decoupler. In the present design, the decoupler thickness is 9 cm, which is a compromise between peak neutronic performance and a thermal-hydraulics requirement to minimize the pressure drop in the coolant loop.

## VI. OPTIMIZATION OF THE LEAD BLANKET

The primary function of the lead blanket is to create an "infinite" target that maximizes neutron production. In such an infinite target, high neutronic efficiency is achieved by distributing $^3$He throughout the blanket region. Optimal neutron production and neutronic efficiency is realized when aluminum structure and, to some degree, coolant in the blanket is minimized.

### A. Lead Blanket Coolant

As with the tungsten neutron source, the two coolants studied for use in the lead blanket region were light water and heavy water. Figure 12 shows the results of a lateral lead thickness study (for a 1-GeV proton beam) in which both light and heavy water were used. The results show clearly that light water performs better than heavy water. Presumably the strong moderating power of hydrogen quickly moderates the neutrons so they bypass the resonance absorption region of lead and are instead captured by $^3$He, whereas deuterium does not do this as efficiently.

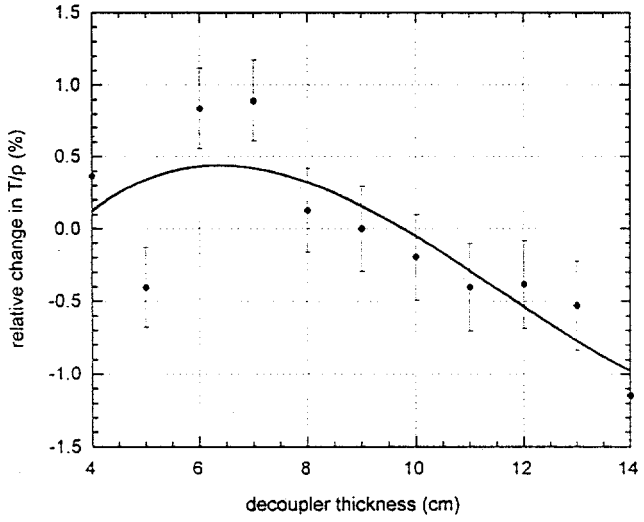


Figure 11. Tritium production versus decoupler thickness.

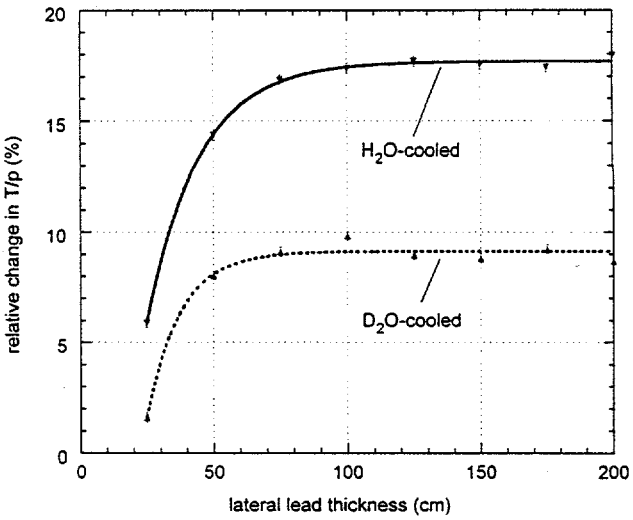


Figure 12. Lateral lead thickness study with light and heavy water coolant.

### B. Coolant Fraction in the Lead

Light water in the lead regions serves two functions: it is a working fluid that cools the lead and aluminum structures, and it is a neutronic moderator that efficiently slows neutrons so they are captured by $^3$He. From a neutronics standpoint, the optimal volume fraction of light water depends on the parasitic absorption properties of neighboring structures, and to a lesser extent on the relative mix of lead, $^3$He, and aluminum in the lead region itself. Figure 13 shows the results of a study (for a 1-GeV proton beam) in which the volume fraction of water was varied over ranges which are reasonable from a thermal-hydraulics viewpoint. For the row 1 lead, tritium

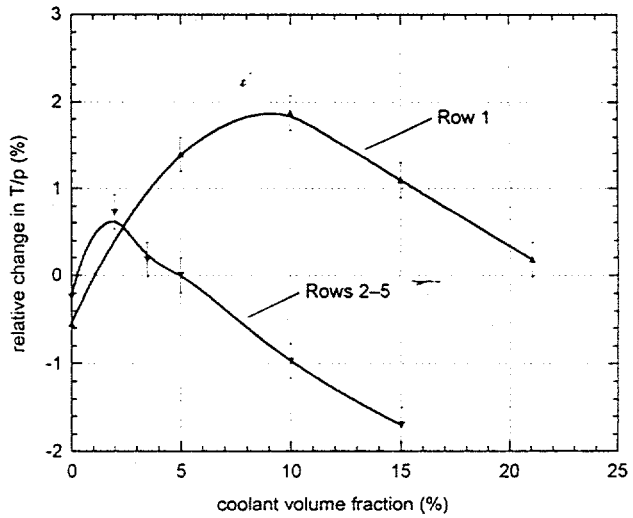


Figure 13. Tritium production rate as a function of light water coolant fraction in the lead regions.

production peaks at a light water volume fraction of about 9%, whereas for the outer rows the production peaks at a much lower fraction, about 2%. The reason the optimum fraction is higher for row 1 is due to its proximity to the decoupler, which has a high volume fraction of $^3$He.

### C. Lateral & Downstream Lead Thickness

The thickness of the lateral lead region is sized such that an "infinite" target is realized. An infinite target is one for which additional lead does not add significantly to the total neutron production, indicating that most high-energy particles that cause spallation are ranged out (the tiny fraction that isn't dominates the shielding problem). Figure 14 shows tritium production as a function of lateral lead thickness for typical lead region composition and a proton beam energy of 1.7 GeV. Beyond 120 cm thickness, the tritium production is constant and there is no neutronic motivation for extending the lead region.

The same neutronics argument drives the thickness of the downstream lead region as well. This study is shown in Figure 15, where an infinite target is achieved by a thickness of 150 cm for realistic lead region compositions.

## VII. NEUTRONIC PERFORMANCE

Table 1 gives a summary of neutron sources and losses in the target/blanket. Overall, about 47 neutrons are produced per proton incident on target. Almost half are produced in the tungsten neutron source region, while the lead blanket and decoupler are responsible for most of the remainder. Of those produced, 84.5% are captured by $^3$He and produce tritium, corresponding to a T/p ratio of nearly 40. Of the remainder, 14% are parasitically captured,

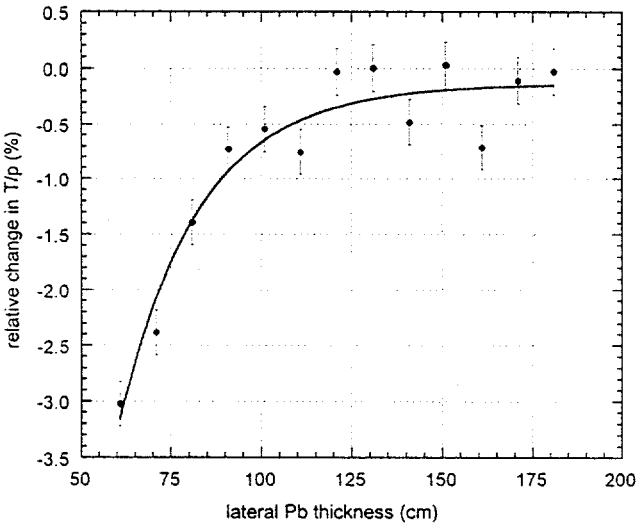


Figure 14. Tritium production versus lateral lead thickness.

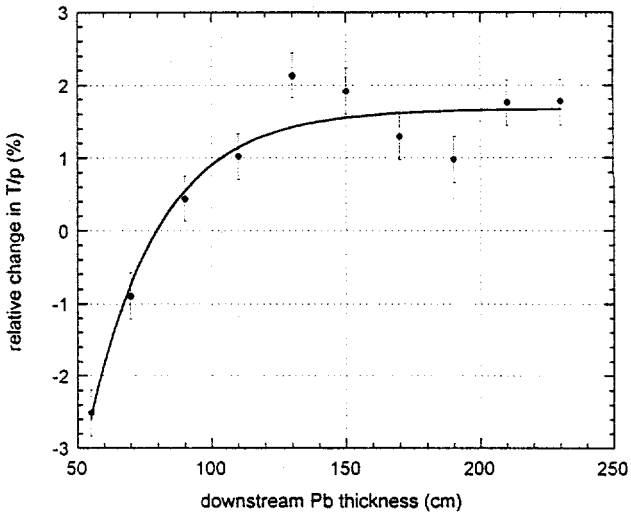


Figure 15. Sensitivity of T/p to downstream lead thickness.

Table 1. Neutron balance sheet for the target/blanket.

| | n/p |
|---|---|
| Neutron sources: | |
| tungsten neutron source | 22.2 |
| lead blanket & decoupler | 24.5 |
| other (window, etc.) | 0.5 |
| Total | 47.2 |
| | |
| Neutron losses: | |
| captures in $^3$He | 39.9 |
| parasitic captures | |
| tungsten neutron source | 3.0 |
| other (Pb, Al, $H_2O$) | 3.5 |
| leakage from system | 0.8 |
| Total | 47.2 |

while nearly 2% leak from the system. The value of n/p is 47.2, which is 75% of the neutron yield from a solid, infinite tungsten target, for which n/p = 63. Further, T/p is 63% of this value, from which we deduce that the APT T/B has an overall neutronic efficiency that is 63% of its theoretical maximum.

Figure 16 shows the tritium production by region. Nearly 36% of the tritium is produced in the decoupler region, where thermal and fast neutron fluxes are high (see Figure 17). Most of the remainder (56%) is produced in rows 1 through 3. Rows 4 and 5 and the reflector regions produce 8% of the total.

The neutron fluxes encountered in the T/B rival the fluxes encountered in the world's most intense research reactors. Figure 17 shows the peak flux as a function of

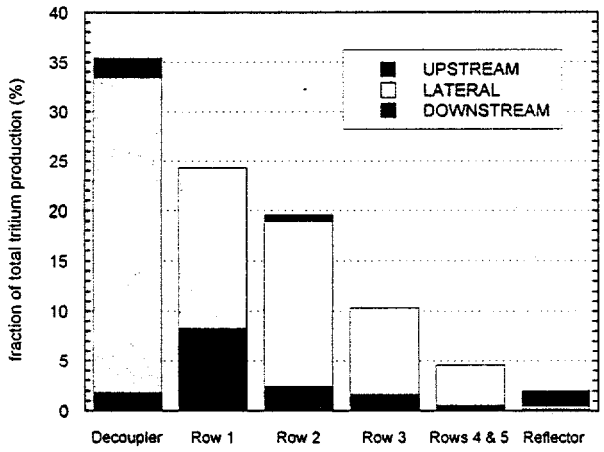


Figure 16. Tritium production by region.

lateral distance as one moves away from beam centerline. The flux is divided into three energy groups, as labeled in the figure. The spectrum is quite hard, as may be expected since thermal neutrons are readily absorbed by the $^3$He prevalent throughout the blanket.

## VIII. ENERGY DEPOSITION IN THE T/B

One of the inherent safety features of the APT concept is that spallation, unlike fission, is an endothermic reaction. For every neutron released from tungsten and lead, about 8 MeV of energy is converted to mass. Of the 170 MW of beam power incident on the target/blanket, only 130 MW is converted to heat that must be carried away. Approximately 38 MW is converted to mass, while the remainder leaks from the system in the form of neutrinos. The breakdown of power deposition among the various regions is shown in Table 2. About half of the total power under normal operating conditions is deposited in the tungsten neutron source. Most of the remainder is deposited in the decoupler and blanket regions surrounding the tungsten neutron source.

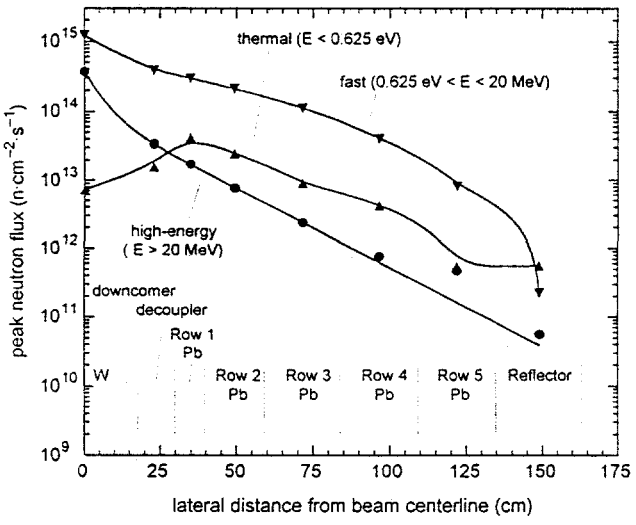


Figure 17. Peak neutron flux as a function of lateral position in the target/blanket.

Table 2. Target/blanket system power distribution at full-power operation.

| Region | Deposited Power, MW |
|---|---|
| Window | 0.6 |
| Tungsten Neutron Source | 64.5 |
| Lateral Decoupler | 14.5 |
| Lateral Blanket Row 1 | 16.1 |
| Lateral Blanket Row 2 | 8.2 |
| Lateral Blanket Row 3 | 2.5 |
| Lateral Blanket Row 4 | 0.8 |
| Lateral Blanket Row 5 | 0.2 |
| Above/below Target | 3.9 |
| Reflector | 0.5 |
| Shield | 2.7 |
| Downstream Blanket | 13.6 |
| Upstream Blanket | 1.4 |
| Total | 129.5 |

## IX. RADIONUCLIDE INVENTORY & DECAY HEAT

The spallation process produces a wide range of nuclear products. Some 2100 nuclides, many of them radioactive, are produced in the target/blanket. The buildup and decay of these radionuclides with time has implications in the areas of safety, licensing, operations, and neutronics performance. With regard to safety, the radionuclide inventory is used as input for determination of accident source terms. Further, the decay heat produced by these radionuclides, while very low compared to the power deposited by the beam, must be dealt with during shutdown and off-normal events.

The inventory of nuclides in the T/B after a single 100-mA, nine-month irradiation at 1.7 GeV has been calculated using the LCS and CINDER'90. This calculation provides a wealth of time-dependent data on radionuclide inventory, decay heat, absorption cross section, and gamma sources in 62 distinct regions of the target/blanket.

The calculated radionuclide inventory is used as input to safety analyses and waste stream characterization. An example of the inventory for the entire T/B after a single nine-month irradiation followed by a five-day cooldown is shown in Table 3. Presented are the top 40 radionuclides, ranked by activity. In all, some 900 radionuclides are

present after five days cooldown. The top 40 radionuclides account for over 88% of the total activity at this time, which is 37.3 MCi. Seven of the top ten radionuclides are tungsten spallation products, while the remaining three ($^{201}$Tl, $^{203}$Pb, and $^{202}$Tl) are lead products. Thus much of the radioactivity is confined to the tungsten.

Figure 18 shows the elemental inventory of the target/blanket relative to the initial inventory five days after a nine-month irradiation. The lower portion of the figure shows that 1 kg of O, 1.8 kg of Al, 200 g of stainless steel, 17 kg of W, and 8 kg of Pb are transmuted. Spallation products span the entire range of elements with atomic numbers below that of Pb, as shown in the upper part of the figure. Most notable is the production of 10 kg of Re. Note the results presented in this figure ignore the depletion of 3 kg of $^{3}$He and the concomitant production of 3 kg of tritium that occurs during the nine-month irradiation.

Table 3. Radionuclide inventory in the target/blanket five days after a nine-month irradiation at 100 mA.

| Radionuclide | Half-life, days | Activity, kCi |
|---|---|---|
| W 185 | 75.1 | 11,200 |
| W 181 | 121 | 4,570 |
| Ta178 | 0.00647 | 1,320 |
| W 178 | 21.6 | 1,320 |
| Tl201 | 3.04 | 1,260 |
| Pb203 | 2.16 | 1,210 |
| Tl202 | 12.2 | 995 |
| Hf175 | 70.0 | 960 |
| W 187 | 0.996 | 861 |
| Yb169 | 32.0 | 834 |
| Re186 | 3.78 | 604 |
| Ta179 | 665 | 589 |
| Au195 | 186 | 579 |
| H 3 | 4500 | 573 |
| Lu171 | 8.24 | 550 |
| Ta183 | 5.10 | 469 |
| Hg197 | 2.67 | 435 |
| Ta182 | 115 | 310 |
| Cr 51 | 27.7 | 307 |
| Ta177 | 2.36 | 286 |
| Tl200 | 1.09 | 278 |
| Lu173 | 500 | 278 |
| Tm167 | 9.24 | 255 |
| Lu172 | 6.70 | 231 |
| Hg203 | 46.6 | 229 |
| Tl204 | 1380 | 222 |
| Re183 | 70.0 | 218 |
| Ir189 | 13.2 | 195 |
| Os185 | 93.6 | 182 |
| Hf172 | 683 | 175 |
| Lu170 | 2.00 | 170 |
| Be 7 | 53.3 | 161 |
| Dy159 | 144 | 157 |
| Eu146 | 4.59 | 156 |
| Eu147 | 24.0 | 155 |
| Mn 54 | 312 | 143 |
| Ir188 | 1.73 | 141 |
| Cs131 | 9.69 | 135 |
| Xe127 | 36.4 | 135 |
| Eu149 | 93.1 | 135 |

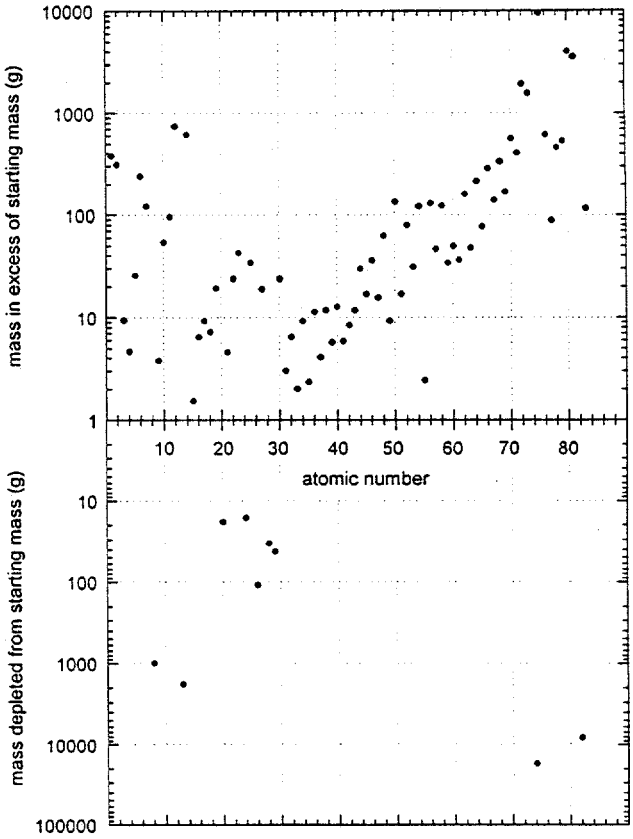


Figure 18. Build-up and burn-up of elements in the T/B five days after a nine-month irradiation at 100 mA.

Figure 19 shows the decay power as a fraction of steady-state power for several representative regions. Immediately after beam turnoff, decay heat generated by the radioactive products is generally on the order of 1% of the steady-state power. After ten days cooldown, most regions have decay powers that are less than 0.1% of their respective steady-state powers.

Since much of the radionuclide inventory resides in the tungsten, the decay power of the tungsten neutron source is an important quantity with repsect to accident analysis. Immediately upon shutdown after a nine-month irradiation, the decay power in all thirteen ladders is 483

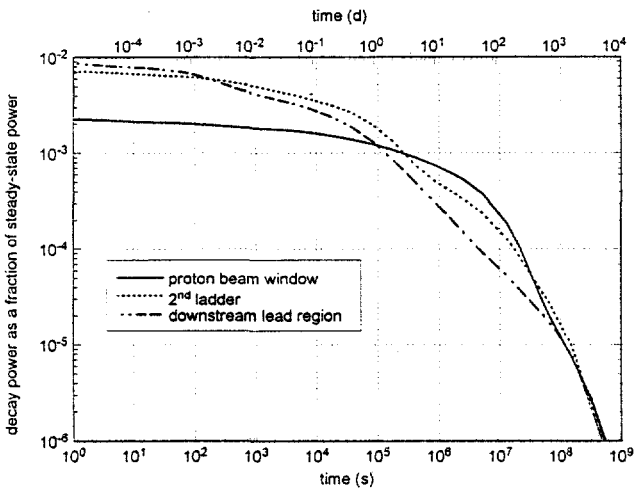


Figure 19. Fractional decay power after beam turnoff for several representative regions of the target/blanket.

kW. This drops to 142 kW after one day, 49 kW after 5 days, and 35 kW after 10 days.

## X. SUMMARY

The present design of the APT target/blanket has been optimized for tritium production within the constraints imposed by engineering, safety, and reliability considerations. For a 1.7-GeV proton beam, the neutron production rate, n/p, is 75% of that achievable with an ideal target, and the neutronic efficiency, T/n, is 84%, leading to an overall tritium production rate of 40 T/p, which is 63% of the theoretical maximum. At a beam current of 100 mA and an overall plant availability of 75%, this production rate translates into 3 kg of tritium produced per year.

## REFERENCES

1. R. E. Prael and H. Lichtenstein, "User Guide to the LCS: The LAHET Code System," Los Alamos National Laboratory Report LA–UR–89–3014, September 1989.

2. J. F. Breismeister, ed., "MCNP—A General Monte Carlo N-Particle Transport Code, Version 4B," Los Alamos National Laboratory Report LA–12625–M, March 1997.

3. W. B. Wilson, et al., "Accelerator Transmutation Studies at Los Alamos with LAHET, MCNP, and CINDER'90," Los Alamos National Laboratory Report LA–UR–93–3080, January 1993.

4. R. B. Kidman, "Tritium Implantation In The Accelerator Production Of Tritium Device," Los Alamos National Laboratory Report LA–UR–97–2464, submitted to these proceedings.